Roles for the Stem Cell–Associated Intermediate Filament Nestin in Prostate Cancer Migration and Metastasis

Wolfram Kleeberger,[1] G. Steven Bova,[1,2,3,4] Matthew E. Nielsen,[2] Mehsati Herawi,[1] Ai-Ying Chuang,[1] Jonathan I. Epstein,[1,2,3] and David M. Berman[1,2,3]

Departments of [1]Pathology, [2]Urology, and [3]Oncology and [4]Health Information Sciences, The Johns Hopkins University School of Medicine, Baltimore, Maryland

Abstract

The intermediate filament protein Nestin identifies stem/progenitor cells in adult tissues, but the function of Nestin is poorly understood. We investigated Nestin expression and function in common lethal cancers. Nestin mRNA was detected in cell lines from small cell lung, and breast cancers, and particularly elevated in cell lines derived from prostate cancer metastases. Whereas the androgen-independent lines PC3, 22RV1, and DU145 all expressed Nestin transcripts under standard culture conditions, the androgen-dependent line LnCaP expressed Nestin only on androgen withdrawal. We confirmed associations of Nestin expression, androgen withdrawal, and metastatic potential by immunohistochemical analysis of samples from 254 prostate cancer patients. Cytoplasmic Nestin protein was readily identifiable in prostate cancer cells from 75% of patients with lethal androgen-independent disease, even in cancer sampled from the prostate itself. However, Nestin expression was undetectable in localized androgen-deprived tumors and in metastases without prior androgen deprivation. To address its function, we reduced Nestin levels with short hairpin RNAs, markedly inhibiting *in vitro* migration and invasion in prostate cancer cells but leaving cell growth intact. Nestin knockdown also diminished metastases 5-fold compared with controls despite uncompromised tumorigenicity at the site of inoculation. These results specify a function for Nestin in cell motility and identify a novel pathway for prostate cancer metastasis. Activity of this pathway may be selected by the extraprostatic environment or, as supported by our data, may originate within the prostate after androgen deprivation. Further dissection of this novel Nestin migration pathway may lead to strategies to prevent and neutralize metastatic spread. [Cancer Res 2007;67(19):9199–206]

Introduction

Cancer cells and stem or progenitor cells share several remarkable properties that set them apart from normal cells. The enhanced capacity of stem/progenitor cells for proliferation, survival, and motility contributes to tissue homeostasis and injury repair, whereas similar abilities are hallmarks of aggressive cancers, distinguishing them from their more indolent counterparts. Little is known about the molecular basis of these distinctive abilities. Further insight is likely to be found in studying genes that distinguish stem cells from differentiated adult cells, particularly intermediate filament proteins, which have emerging roles in all of these abilities (1). Perhaps, the best characterized of these is the cytoskeletal intermediate filament protein Nestin.

First identified as a marker of neuroepithelial stem/progenitor cell in the brain (2), and also expressed in brain tumors (3, 4), Nestin expression is now known to characterize cancer cells (3, 5–7) and benign stem/progenitor cells (8, 9) in a variety of lineages and to be induced during stem cell activation in response to tissue injury (10–13). The known link between chronic injury repair and cancer risk has been proposed to act through activation of tissue stem cells (14) and be relevant to prostate carcinogenesis (15). Nestin is therefore of particular interest in that it has the potential to provide a molecular explanation for this link.

Prostate cancer is very common in developed countries and is widely variable in clinical course. Most cases remain confined to the prostate and adjacent soft tissue and cause no harm. However, approximately one in eight cases metastasizes widely, typically to bone, adjacent soft tissue, liver, and lung (16). Like the organ in which it arises, prostate cancer growth and survival are supported by androgenic hormones. Widely metastatic cases are therefore treated by androgen deprivation therapy (ADT). ADT can be achieved surgically by castration or pharmacologically by suppression of the pituitary-gonadal axis and/or antagonism of the androgen receptor (AR; refs. 17–19). The response to ADT includes reduced tumor bulk and a variable pause in growth that can last several months or even years (19). During this pause, ADT-resistant cells are thought to adapt to growth under lower levels of circulating androgen through a variety of poorly understood changes. Proposed cellular adaptations include (*a*) local synthesis of androgen, (*b*) decreased requirement for androgen through ligand-independent or ligand-promiscuous activation of AR, and (*c*) alterations in growth-regulatory networks that signal between tumor and adjacent stromal cells (17–19). The observation that castration is never curative and the heterogeneous ability of cells within prostate tumors to support growth on castration suggest that ADT-resistant or "castration-resistant" subpopulations of prostate cancer cells exist before ADT (19, 20). Similar heterogeneity with regard to ADT resistance is also seen in benign prostate epithelium. Most prostate epithelium involutes in response to ADT but can be reconstituted by ADT-resistant epithelial stem cells on androgen replacement (21). This ADT-resistant stem cell–like phenotype is the primary culprit in prostate cancer morbidity and mortality, particularly in metastatic prostate cancer. Our study focuses on the expression and function of Nestin in this subset of prostate cancer cells.

The function of Nestin is unclear, but clues may be gleaned from studies of related proteins. Cytoskeletal intermediate filament proteins are critical and dynamic structural elements whose

Note: Supplementary data for this article are available at Cancer Research Online (http://cancerres.aacrjournals.org/).

Requests for reprints: David M. Berman, The Johns Hopkins University Medical School, 1550 Orleans Street, CRB2 Room 545, Baltimore, MD 21231. Phone: 443-287-0878; Fax: 410-502-5742; E-mail: berman@jhmi.edu.

doi:10.1158/0008-5472.CAN-07-0806

assembly and disassembly influence and respond to intracellular signaling cascades that control a variety of critical processes, including proliferation, migration, and survival (1). These dynamics are illustrated (*a*) by the role of Nestin as a substrate for phosphorylation on Thr^{316} by cdc2 kinase that occurs in association with cytoplasmic reorganization during mitosis (22); (*b*) by Nestin-mediated facilitation of mitosis-associated disassembly of vimentin, another intermediate filament protein with which Nestin copolymerizes (23, 24); and (*c*) by the Nestin-dependent sequestration and inactivation of cyclin-dependent kinase 5, a proapoptotic kinase in the nervous system (25). These and other observations suggest that Nestin may serve as a central organizer of several processes important to cancer. Here, we show increased levels of Nestin in common lethal carcinomas, particularly in the most aggressive forms of prostate cancer. In these tumors, we show novel functions for Nestin in cell migration and in prostate cancer metastasis.

Materials and Methods

Cell culture. Human cancer cell lines were obtained from the American Type Culture Collection and maintained in RPMI 1640 supplemented with 10% fetal bovine serum (FBS), except MCF7 and HCT116, which were maintained in DMEM/10% FBS and McCoy's/10% FBS respectively. Prostate epithelial cells (PrEC; Cambrex Biochemicals) were cultured according to the vendor's instructions. AT6.3 cells were provided by Dr. John T. Isaacs (The Sidney Kimmel Comprehensive Cancer Center and the Brady Urological Institute, The Johns Hopkins University School of Medicine, Baltimore, MD) and maintained in RPMI 1640 supplemented with 10% FBS and 250 nmol/L dexamethasone. NRP152 cells were provided by David Danielpour (Case Cancer Center Research Laboratories, Cleveland, OH) and cultured as described (26). For the androgen withdrawal experiments, LnCaP cells were cultured in RPMI 1640 supplemented with 10% charcoal-stripped FBS (Biomeda) for 72 h. To ensure reproducibility, these experiments were repeated and done in triplicate.

Tissue specimens. Formalin-fixed, paraffin-embedded tissue samples from ADT-naive patients were obtained from the archives of the Department of Pathology, Johns Hopkins University School of Medicine. Tumor tissue from patients that had died from lethal metastatic prostate cancer was obtained through a rapid autopsy program done by the PELICAN laboratory devoted to integrated studies of metastatic prostate cancer. All of these patients had received ADT prior to death.

A total of 124 cases of ADT-naive localized prostate carcinoma derived from radical prostatectomies and 46 cases of ADT-naive metastases was distributed among five tissue microarrays (TMA) with each case represented by at least three spots. The metastases consisted of regional lymph node deposits ($n = 43$) and soft tissue lesions ($n = 3$). Another TMA was constructed to contain all tissue specimens available from 32 lethal cases (i.e., patients who died with widespread metastatic prostate cancer). All lethal cases were treated with ADT at some time in their disease course. Tumor was harvested at autopsy and represented by one spot per lesion. Lastly, we constructed a further TMA that contained ADT-treated localized tumor samples from 52 patients treated briefly (usually 1–6 months) with a luteinizing hormone-releasing hormone agonist before sampling at radical prostatectomy. On evaluation by an expert genitourinary pathologist (D.M.B.), all of these cases showed histologic features of ADT. Clinicopathologic details for all cases are described in Supplementary Tables S1 and S2.

Immunohistochemistry and immunofluorescence. Sections (5 μm) were cut from TMAs, deparaffinized, rehydrated, and subjected to heat-induced antigen retrieval in citrate buffer (pH 6.0) for 20 min at 90°C. Nonspecific binding sites were blocked with serum-free blocking reagent (DAKO) and anti-Nestin antibodies (antihuman clone 10C2 at 1:5,000 or antirodent clone RAT401 at 1:500; both from Chemicon) were applied for 1 h at 25°C. Immunodetection was carried out with horseradish peroxidase (HRP)-conjugated rabbit anti-mouse (1:500; DAKO) for 30 min and a tyramide signal amplification kit according to the manufacturer's instructions (TSA Indirect, Perkin-Elmer Life Sciences). 3,3′-Diaminobenzidine was then used as the visualizing substrate. Finally, sections were counterstained with hematoxylin. The percentage of Nestin-positive tumor cells per lesion was determined by semiquantitative assessment of two representative high-power fields (40× objective) for each TMA spot. To rule out false-positive staining due to unspecific binding of antibodies, we did controls where the primary antibody was substituted by isotype-matched IgG.

For immunofluorescence, cells were cultured on coverslips, fixed in formalin for 5 min at room temperature, and permeabilized in PBS/0.5% Triton X-100 for 10 min. After blocking and incubation with primary antibodies (1:100 for human Nestin), detection was carried out by incubation with Alexa Fluor 488–conjugated antimouse IgG (Invitrogen) for 1 h at room temperature and counterstained on mounting with Vectashield/4′,6-diamidino-2-phenylindole medium (Vector Laboratories). The presentation of staining data in this study conforms to the minimum information specification for *in situ* hybridization and immunohistochemistry experiments (MISFISHIE) standard for reporting gene expression localization experiments (27).

Real-time reverse transcription-PCR analysis. Total RNA was isolated with the RNeasy Mini kit (Qiagen) and random-primed cDNA was synthesized using Ready-To-Go You-Prime First-Strand Beads (GE Healthcare). The volume of the first-strand reaction was brought to 300 μL with water and 5 μL were amplified on an iCycler (Bio-Rad) using iQ SYBR Green Supermix (Bio-Rad) and gene-specific oligonucleotide primers. All PCRs were done at 95°C for 5 min followed by 40 cycles of 15, 30, and 30 s at 95°C, 60°C, and 75°C, respectively. Bio-Rad software was used to calculate threshold cycle (*C*T) values for all target genes and for the reference gene *hypoxanthine phosphoribosyltransferase* (*HPRT*). The expression values for the tumor cell lines (tumor sample) are presented as fold expression in relation to a benign cell line (control sample); the actual values were calculated using the $2^{-\Delta\Delta CT}$ equation, where $\Delta\Delta C\mathrm{T} = [C\mathrm{T}_{\mathrm{Target}} - C\mathrm{T}_{\mathrm{Hprt}}]_{(\mathrm{TUMOR\ SAMPLE})} - [C\mathrm{T}_{\mathrm{Target}} - C\mathrm{T}_{\mathrm{Hprt}}]_{(\mathrm{CONTROL\ SAMPLE})}$. The following primer sequences were used: human and rat HPRT (5′-CTTTGCTGACCTGCTGGATT-3′ and 5′-GTTGAGAGATCATCTCCACC-3′), human Nestin (5′-CTGCGGGCTACTGAAAAGTT-3′ and 5′-AGGCTGAGGGACATCTTGAG-3′), and rat Nestin (5′-AGAGAAGCGCTGGAACAGAG-3′ and 5′-TTCCAGGATCTGAGCGATCT-3′).

Immunoblotting. Samples (20 μL) of total protein lysates in Mammalian Protein Extraction Reagent (Pierce) were separated by gradient SDS-PAGE and transferred to polyvinylidene difluoride membrane. Nonspecific binding sites were blocked with casein solution (Vector Laboratories). Primary antibodies were mouse anti-Nestin (clone 25; 1:500; BD Transduction Laboratories), mouse anti-vimentin (clone V9; 1:4,000; NeoMarkers), mouse anti-E-cadherin (clone 36; 1:1,000; BD Transduction Laboratories), and mouse anti-glyceraldehyde-3-phosphate dehydrogenase (clone 6C5; 1:5,000; Santa Cruz Biotechnology). The membrane was incubated sequentially with primary antibodies (overnight at 4°C), HRP-conjugated antimouse antibody (1:5,000; Santa Cruz Biotechnology), and chemiluminescent substrate (Pierce) before exposure to film.

Generation of stable small interfering RNA–expressing transfectants. Plasmid vectors (pSM2) encoding the following microRNA-adapted short hairpin RNAs (shRNA; shRNAmirs), 5′-TGCTGTTGACAGTGAGCGCGGATTGTGAACCATCTAGAAATAGTGAAGCCACAGATGTATTTCTAGATGGTTCACAATCCTTGCCTACTGCCTCGGA-3′ (mouse Nestin), 5′-TGCTGTTGACAGTGAGCGCGGCTAGTCCCTGCCTGAATAATAGTGAAGCCACAGATGTATTATTCAGGCAGGGACTAGCCATGCCTACTGCCTCGGA-3′ (human Nestin shRNA1), and 5′-TGCTGTTGACAGTGAGCGAGGCAGACATCATTGGTGTTAATAGTGAAGCCACAGATGTATTAACACCAATGATGTCTGCCCTGCCTACTGCCTCGGA-3′ (human Nestin shRNA2), were purchased from Open Biosystems. These plasmids or a construct containing a scrambled shRNA sequence (control shRNA; Open Biosystems), were stably transfected into AT6.3 or PC3 cells, respectively, using Fugene (Roche Applied Science) according to the manufacturer's instructions. Seventy-two hours later, positive cells were selected in puromycin (5 μg/mL).

Migration and invasion assays. For the wound closure assay, cells were seeded in T6-well culture dishes at a density of 1×10^6 per well. On the next

day, live cells were stained with 1.5 μmol/L calcein (Invitrogen) and a wound was created by scratching a pipette tip through the center of the dish. Images of the wounded areas were taken on a fluorescent microscope at 0 and 36 h. *In vitro* migration and invasion assays using a modified Boyden chamber technique were carried out as described (28), except that AT6.3 cells were plated at 5×10^4 per well and that uncoated inserts (Costar Transwell, Corning) were used to assay for migration. All assays were done in triplicate and at least five high-power fields (20× objective) were counted on each membrane. The number of counted cells was normalized to the viable cell mass on both sides of the membrane.

Cell growth and anchorage-independent growth assays. To assay for *in vitro* proliferation, cells were plated at a density of 2×10^3 in triplicate in 96-well plates. Viable cell mass was determined by absorbance measurements at 490 nm (A490) at 4 consecutive days using the CellTiter96 colorimetric assay (Promega). Anchorage-independent growth was examined by doing a soft agar cloning assay. First, T6-well culture dishes were layered with 0.6% noble agar in growth medium. Then, the trypsinized cells were resuspended in 0.4% agar at a dilution of 5×10^3 per well in triplicate and poured on top of the 0.6% agar. After incubating for 10 days, the colonies were fixed and stained with PBS containing 0.1% Triton X-100, 4% paraformaldehyde, and 1 μg/mL ethidium bromide for 2 days at 4°C, visualized on a UV transilluminator, and counted.

Xenografts and *in vivo* metastasis assay. PC3 or LnCaP cells (1×10^7) in 0.2 mL Matrigel (BD Biosciences) or 1×10^5 AT6.3 cells in 0.2 mL PBS were injected s.c. into the flank of 3- to 4-week-old female athymic *nu/nu* mice (Harlan). Tumors were harvested at a diameter of 5 mm, fixed in formalin, and embedded in paraffin. Tumor volumes were calculated using the formula length × width × depth × $\pi/6$ (29). Lungs were processed for histology and intrapulmonary metastases were counted for one representative section per mouse.

Results

Nestin expression in carcinoma cell lines. Nestin expression has been observed in cell lines from small cell lung and prostate cancer (28, 30) and in a transgenic mouse prostate cancer model (31). We investigated the expression status of Nestin in a more comprehensive panel of carcinoma cell lines from different organs. Specifically, we did a semi-quantitative real-time reverse transcription-PCR (RT-PCR) analysis on a total of 19 cDNAs from prostate, breast, lung, colon, and bladder cancer cell lines. Among these, only cell lines from prostate, breast, and small cell lung cancer showed detectable levels of Nestin mRNA (Fig. 1*A*). These levels were particularly elevated in androgen-insensitive prostate cancer lines (PC3, DU145, and 22RV1), whereas they were undetectable in androgen-dependent LnCaP cells (Fig. 1*A* and *B*). Nestin mRNA levels in LnCaP cells were induced within 72 h of androgen withdrawal, although levels were only approximately one sixth of those seen in PC3 cells (Fig. 1*A*). These results link Nestin expression in prostate cancer to androgen withdrawal.

Nestin expression in clinical specimens. Prostate cancer cell lines are all derived from patients with widespread metastatic disease and thus represent a small but important minority of patients. To better understand the biological and clinical context in which Nestin might operate, we assayed its expression in clinical prostate cancer samples from 254 patients encompassing the entire clinical spectrum of the disease (Supplementary Tables S1 and S2). The one known exception of the restriction of Nestin to stem/progenitor cells in normal adult tissues is its expression in benign endothelial cells (32), which provides a convenient internal control for immunohistochemical studies. Accordingly, we deemed cases with endothelial Nestin expression (89% of cases) as informative. All subsequent references to Nestin expression in clinical cases will pertain to cytoplasmic immunohistochemical staining in prostate cancer cells.

Nestin expression identifies ADT-resistant lethal prostate cancer. Somewhat surprisingly, we found Nestin expression exclusively in lethal cases after treatment with ADT. In ADT-treated men (n = 32; ref. 16) who died with metastatic prostate cancer, 24 (75%) showed readily detectable Nestin protein in the cancer cells (Table 1; Fig. 2*C* and *D*). Staining was variable within cases and within metastatic deposits. In most cases, we detected Nestin-expressing cancer cells in all of the metastatic deposits examined. Within such lesions, the percentage of Nestin-expressing tumor cells varied from 20% to 95% of the cancer cells; the median percentage of all positive lesions was 52%. Given the strong association we observed between Nestin and lethal metastasis, we were surprised to find no detectable Nestin in ADT-naive prostate cancers, including high-grade tumors and lymph node metastases (Table 1; Fig. 2*A* and *B*). Patients with high-grade tumors (Gleason sum 8–10 and those with ductal morphology, n = 90) have a significant (~25–50%) chance of eventual death due to prostate cancer (33), and with limited follow-up of these Nestin-negative ADT-naive cases, we identified 14 who progressed to widespread metastasis within 1 to 9 years of surgery, 5 of whom ultimately died of the disease. Thus, rather than an early marker of metastatic potential or lethality, Nestin expression seems to evolve along with ADT-resistant metastasis.

Nestin expression evolves with advanced disease. This evolution was further supported by a lack of Nestin immunoreactivity in localized (nonmetastatic) tumors from patients (n = 52) with localized prostate cancer who had been subjected to ADT before prostatectomy (Table 1). This result contrasts with the rapid (72 h) induction of Nestin expression in metastasis-derived LnCaP cells (Fig. 1*A*) and further supports the concept that Nestin expression evolves with advanced disease in the setting of ADT. This concept was specifically confirmed in paired metastatic and primary tumors from (*a*) ADT-naive prostates surgically removed in patients who later died of metastatic castration-resistant cancer and (*b*) previously unresected primary cancers sampled *in situ* at the time of death. Of the 11 lethal cases for which matched primary and metastatic lesions were sampled at the time of death, 7 showed Nestin expression in both locations, whereas the remaining 4 showed Nestin expression in neither (Table 1). Conversely, four cancers were Nestin negative when sampled before androgen deprivation yet gave rise to Nestin-positive metastases in the same patients several years later. Taken together, our data indicate that Nestin expression is not induced by environments outside the prostate, nor by ADT alone, but is part of a cellular program that evolves in the prostate itself within months or years of androgen deprivation and is associated with cancer lethality.

Nestin requirement in cell migration but not in cell growth. To test potential functions of Nestin in metastasis, we stably transfected human prostate cancer metastasis-derived PC3 cells with plasmids encoding shRNAs targeting the Nestin transcript or scrambled shRNA control plasmids. Cancer metastasis is associated with increases in growth rate and in cell motility, and both are important characteristics of stem/progenitor cells that could potentially be influenced by intermediate filament protein dynamics. We therefore paid particular attention to these variables in assaying control and Nestin knockdown cells. One of two Nestin shRNA sequences (hNestin shRNA1) dramatically reduced the expression of Nestin protein (Fig. 3*A*), but loss of Nestin had no noticeable effect on cell viability or growth rate (Supplementary

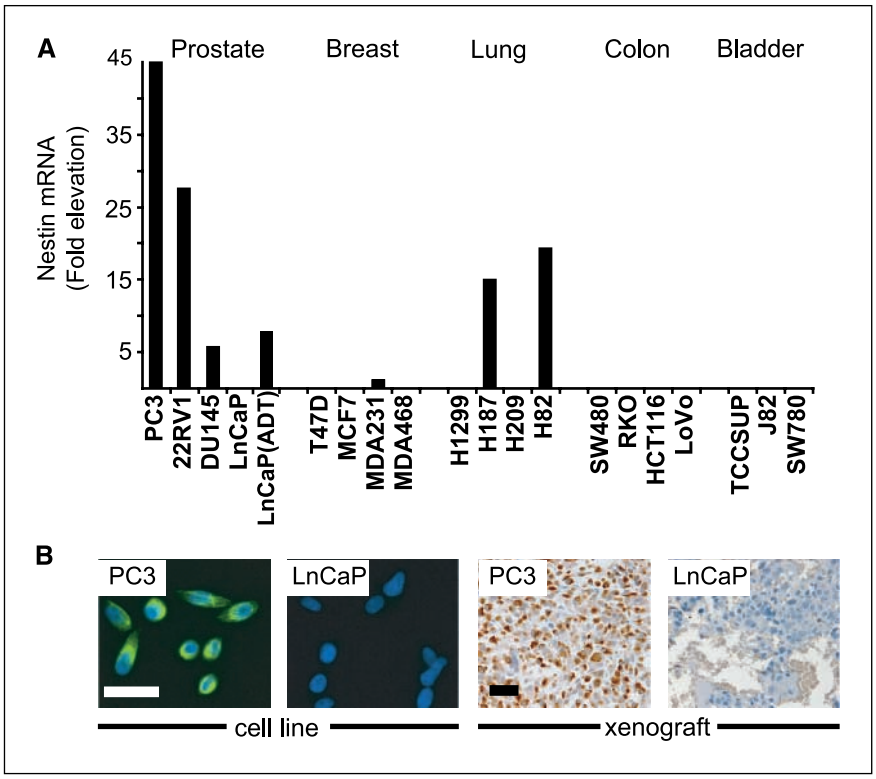

Figure 1. Nestin expression in carcinoma cell lines. *A,* real-time RT-PCR of Nestin transcripts in carcinoma cell lines from five different tissues. Values represent fold elevation above benign human PrEC. *LnCaP(ADT)* labels LnCaP cells that were subjected to androgen withdrawal in culture for 72 h. *B,* photomicrographs showing differential expression of Nestin protein in PC3 and LnCaP cultures and tumor xenografts. *Bar,* 50 μm.

Fig. S1*A*). In contrast, Nestin knockdown greatly reduced cell motility, as indicated by dramatically retarded performance in a wound healing assay *in vitro* (Fig. 3*B*), as well as greatly impaired migration through 8-μm filter pores and invasion through a collagen matrix (modified Boyden chamber assays; Fig. 3*C* and *D*). These effects were dependent on Nestin knockdown, as they were not observed when cells were transfected with plasmids encoding control scrambled shRNA (Fig. 3*C* and *D*) nor with a cognate shRNA (hNestin shRNA2) that failed to suppress Nestin expression (data not shown). These data indicate a specific role for Nestin in cell motility and specify a potential role for Nestin in metastasis.

Table 1. Nestin protein expression and prostate cancer stage

	Total *n*	Nestin, detectable (%)	Nestin, undetectable (%)
ADT-naive cases			
Localized tumors	124	0 (0)	124 (100)
Metastatic lesions	46	0 (0)	46 (100)
ADT-treated cases			
Localized tumors	52	0 (0)	52 (100)
Lethal metastatic cases (castration resistant)			
Patients	32	24 (75)	8 (25)
Metastatic lesions	113	84 (74)	29 (26)
Primary tumors at autopsy	11	7 (64)	4 (36)
Preandrogen ablation tumor tissue*	4	0 (0)	4 (100)

*ADT-naive samples in men who later developed Nestin-positive castration-resistant metastases.

Association of Nestin with a mesenchymal phenotype in highly metastatic AT6.3 prostate carcinoma cells. Because human prostate cancer cell lines have very limited metastatic ability in animal models, we studied Nestin in highly metastatic AT6.3 rodent prostate cancer cells (28, 34). A few weeks after s.c. inoculation, these cells form numerous metastases throughout the body of the host with the lungs being the most prominent site of metastasis. By comparison with benign immortalized NRP152 rat PrECs (26), AT6.3 cells express features of epithelial to mesenchymal transition, including loss of the epithelial adhesion protein E-cadherin and gain of the intermediate filament protein vimentin (Fig. 4*C*; ref. 1). Coexpression of vimentin likely facilitates Nestin function, as Nestin, unlike other intermediate filament proteins, cannot form homopolymers but rather must heteropolymerize with other intermediate filament proteins (23). As seen previously (28), s.c. AT6.3 xenografts grew rapidly at the site of inoculation and frequently metastasized to the lungs (Fig. 4*B*). Intriguingly, although abundant Nestin expression was observed in AT6.3 cells and s.c. xenografts (Fig. 4*A* and *B*), we observed substantial enrichment for cells with high-level Nestin expression in metastases, particularly in micrometastases (compare photomicrographs in Fig. 4*B*), suggesting a role for Nestin in colonizing metastatic sites.

To evaluate the function of Nestin in metastasis, we targeted Nestin expression with a rat-specific shRNA (rNestin shRNA) in AT6.3 cells. This sequence effectively reduced Nestin protein expression but had no appreciable effect on vimentin or E-cadherin

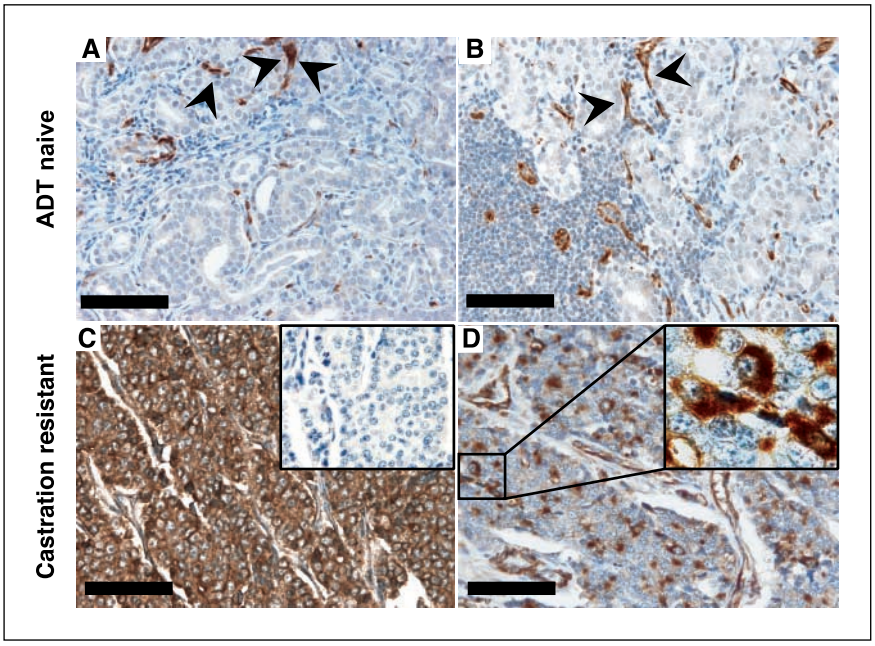

Figure 2. Nestin expression identifies lethal prostate tumors. Photomicrographs showing a ADT-naive localized tumor with no metastasis at time of surgery (*A*), a ADT-naive regional (pelvic) lymph node metastasis (*B*), as well as two metastatic lesions from castration-resistant lethal prostate cancer cases displaying a high percentage (95%; *C*) versus a low percentage (20%; *D*) of Nestin-positive tumor cells. *C, inset,* no positivity was detectable in the corresponding IgG control stainings that were done to rule out unspecific labeling of tumor cells. *D, inset,* high magnification showing cytoplasmic Nestin staining in cancer cells. Nestin-positive small blood vessels were seen in all samples (*arrowheads*) and served as a positive internal control for staining quality but were still clearly distinguishable from positive tumor cells at high-power magnification. Nestin staining in tumor cells was detected only in lethal cases. *Bar*, 100 μm.

(Fig. 4*C*). Assays of *in vitro* growth and invasion in rodent AT6.3 cells (Fig. 4*D*) confirmed the migration defects and unaffected growth rates observed in human prostate cancer cells (Fig. 3; Supplementary Fig. S1). These data, derived from the use of independent shRNAs targeting separate sequences in rodent and human cell lines, exclude off-target RNA interference effects as the basis for our observations and confirm a novel role for Nestin in cell migration.

Nestin is required for AT6.3 prostate cancer metastasis. We inoculated athymic mice with s.c. xenografts containing Nestin-targeted or control AT6.3 cells. At the site of inoculation, both types of xenografts grew at equivalent rates (Fig. 5*A*). However, examination of the lungs at 4 weeks after inoculation revealed that, in comparison with control tumors, Nestin-targeted tumors produced approximately one fourth the number of metastatic deposits and these deposits were dramatically reduced in size (Fig. 5*B* and *C*). In light of our observations linking Nestin expression to widely metastatic human prostate cancer (Table 1; Figs. 1 and 2), these data indicate a role for Nestin-mediated migration in human prostate cancer lethality and metastasis.

Discussion

These studies indicate a requirement for Nestin in cell migration and significantly expand our understanding of Nestin function.

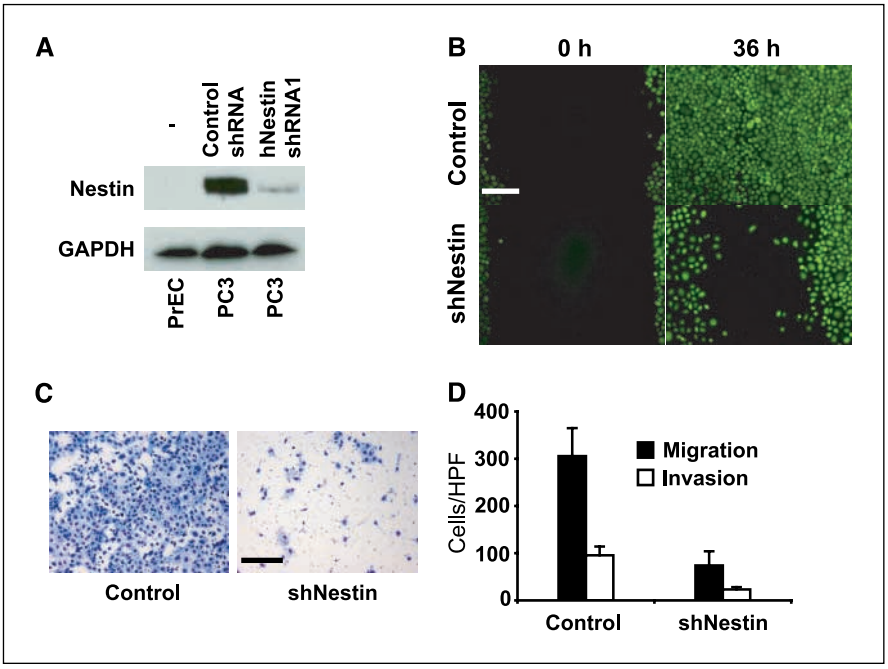

Figure 3. Nestin enhances prostate cancer cell motility. *A,* Western blot showing diminished Nestin protein levels in human PC3 prostate cancer cells stably transfected with a shRNAmir construct targeting human Nestin (*hNestin shRNA1*) when compared with the same cells stably transfected with a scrambled control shRNA construct (*Control shRNA*). Untransfected (−) benign human PrECs lack detectable Nestin protein. *GAPDH,* glyceraldehyde-3-phosphate dehydrogenase. *B,* wound healing assay of calcein-stained (*green*) PC3-control and PC3-siNestin cells. Thirty-six hours after wounding, control cells completely cover the denuded area of the plate, whereas "healing" is markedly inhibited in PC3-siNestin cells. Representative photomicrographs are shown from one of three comparable experiments. *Bar*, 100 μm. *C,* photomicrographs of a modified Boyden chamber assay showing that numerous PC3-control cells (*left*) but only few PC3-siNestin cells (*right*) traverse an uncoated porous membrane after 20 h. *Bar*, 100 μm. *D,* number of cells migrating through uncoated membranes or invading through Matrigel-coated membranes in modified Boyden chamber assays ($P < 0.0001$). All Boyden chamber assays were done in triplicate. *HPF,* high-power field. *Columns,* mean; *bars,* SD.

In prostate cancer, we further link this role to androgen deprivation and lethality in human samples and show its requirement in a rodent model of lethal metastasis. Because previous studies have established Nestin expression as a property of immature stem/progenitor cells, our results raise interesting questions about the role of Nestin in immature cells and the origins of Nestin expression in the prostate.

Unlimited replicative potential is the cardinal property of stem cells; we were therefore surprised that Nestin knockdown had no demonstrable effect on cell growth. Indeed, previous studies have linked Nestin to the cell cycle by showing Nestin-mediated disassembly of intermediate filament proteins in mitotic cells, although no effect on proliferation was reported (23). One possible explanation for these findings is that Nestin is one of several intermediate filaments that permits rapid proliferation but is not required for it. Alternatively, the cancer cells used in our studies may have overcome a requirement for Nestin in proliferation that remains intact in benign cells.

In contrast to proliferation, migration was greatly enhanced by Nestin in human and rodent prostate cancer cells. Cell migration is a multistep process that includes the extension of lamellopodia through actin polymerization and the coordinated formation and disassembly of focal adhesion complexes (35, 36). There is increasing evidence that intermediate filament proteins are involved in cell migration. For example, augmenting vimentin levels has been shown to promote motility and metastatic potential (37, 38). In addition, synemin, an intermediate filament protein structurally similar to Nestin, can bind to α-actinin and vinculin (39), which participate in cell movement through interactions with actin and focal adhesions, respectively. Our initial examination of the morphology, localization, and number of lamellopodia and focal adhesions and of actin distribution did not reveal any definitive differences between control and Nestin-targeted cells (data not shown). Further studies will be needed to identify additional members of the migration pathway in which Nestin participates and to elucidate their roles.

Our study identifies a pathologic role for Nestin in prostate cancer. However, a physiologic context for Nestin in the prostate remains to be characterized. In the pancreas, another gut-derived glandular organ, Nestin expression marks epithelial precursor cells, both in the embryo (40) and in epithelial metaplasia, a common response to epithelial injury (41). In the prostate, Doles et al. (42) reported expression of Nestin mRNA in the preliminary budding stage of embryonic development and found that decreased expression of Nestin in Gli2-null transgenic mice was associated with aberrantly placed prostate epithelial buds. Thus, Nestin may act in cell movements that pattern the early prostate and become reactivated in injured and/or metaplastic prostate as it is in other injured tissues (10–13). The known link between chronic injury repair and cancer risk has been proposed to act through activation of tissue stem cells (14) and be relevant to prostate carcinogenesis (15).

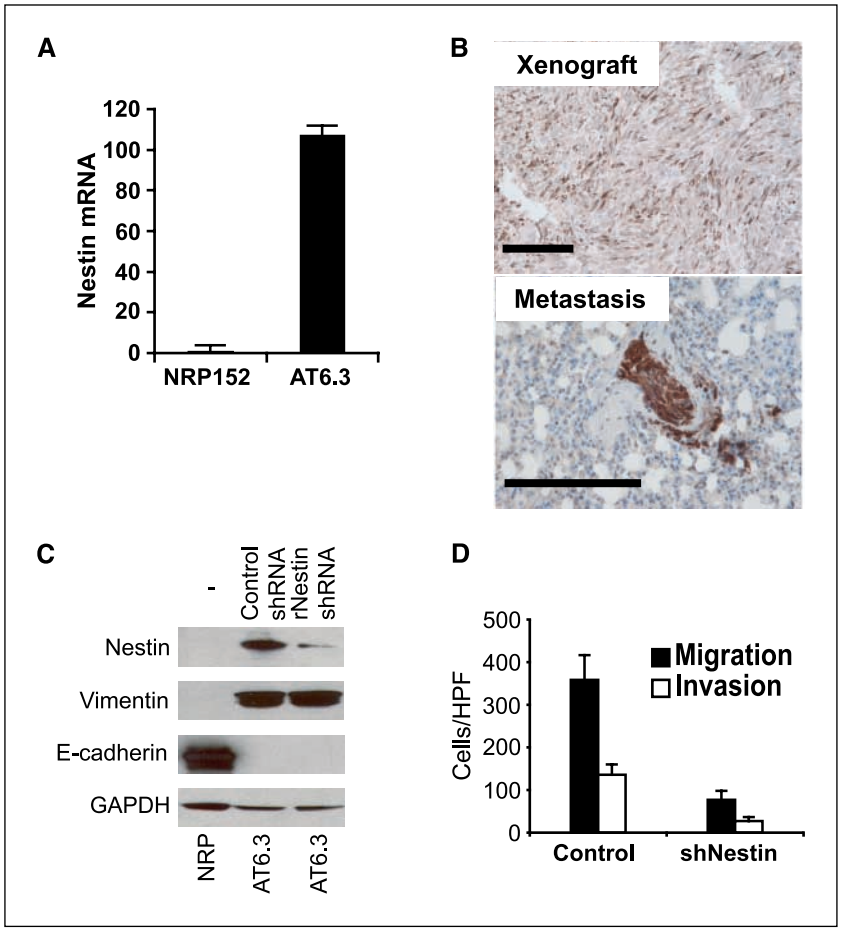

Figure 4. Nestin knockdown in rodent AT6.3 prostate carcinoma cells impairs cell motility. *A,* real-time RT-PCR showing that Nestin mRNA levels are >100-fold higher in AT6.3 cells compared with benign rat PrECs (NRP152). *Columns,* mean; *bars,* SD. Assays were done in triplicate. *B,* immunohistochemistry shows heterogeneous expression of rat Nestin in an AT6.3 xenograft at the site of inoculation. In contrast, ~100% of the AT6.3 cells in an intrapulmonary micrometastatic lesion stain positive. *Bar*, 100 μm. *C,* Western blot showing near-complete knockdown in AT6.3 cells stably transfected with a shRNAmir construct targeting rat Nestin (*rNestin shRNA1*) when compared with the same cells stably transfected with a scrambled control shRNA construct (*Control shRNA*). Untransfected (–) benign rat PrECs (*NRP*) lack detectable Nestin protein. Expression of the epithelial to mesenchymal transition–associated markers vimentin and E-cadherin is not affected. *D,* modified Boyden chamber assays show marked decrease in migratory and invasive ability in AT6.3-siNestin cells ($P < 0.0001$). Assays were done in triplicate.

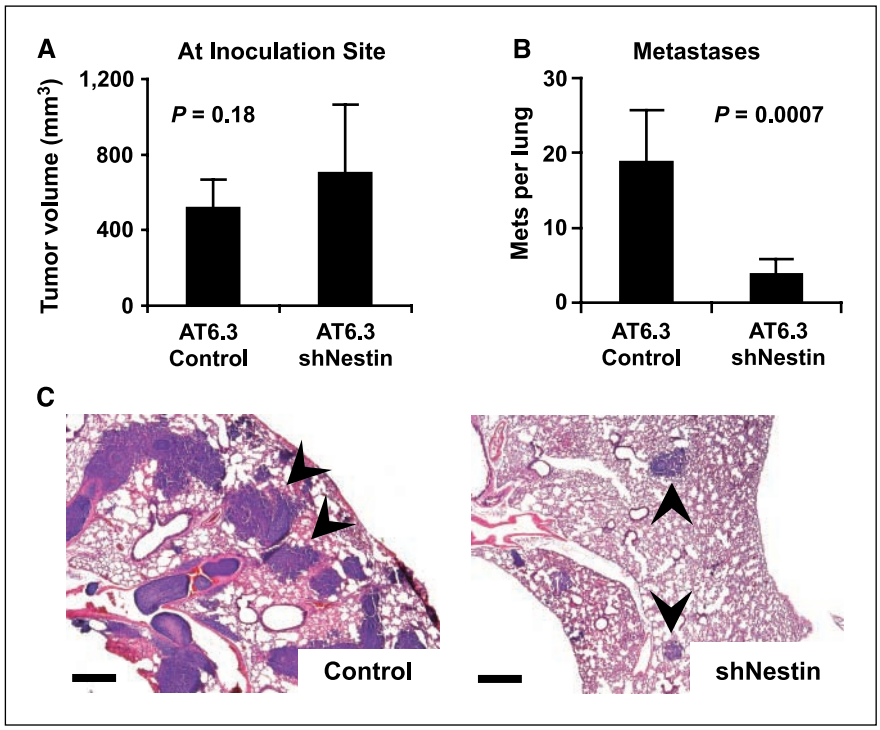

Figure 5. Nestin requirement in AT6.3 prostate cancer metastasis. *A,* at the site of inoculation, xenograft tumors derived from AT6.3-control and AT6.3-siNestin cells show no significant difference in tumor volume after 4 wks. *B,* counting the number of macrometastatic lesions per one representative cross-section of the lungs from each mouse in *A* reveals a dramatic decrease in metastatic ability in the AT6.3-siNestin cells. *Columns,* mean (n = 9); *bars,* SD. *C,* photomicrographs showing representative sections of the lungs from both groups. *Arrowheads,* intrapulmonary metastatic lesions are visible as blue nodules. Note marked reduction in size as well as the number of metastases in the AT6.3-siNestin group (sections are stained with H&E). *Bar*, 500 μm.

Future studies addressing Nestin expression in prostate progenitor cells have the potential to provide a molecular explanation for this link.

We detected Nestin expression exclusively in androgen-independent lethal prostate cancers, where it was present at the site of origin (the prostate) and in distant metastases. In contrast, ADT-naive tumors lacked detectable Nestin expression but seemed to convert to high levels of Nestin expression during progression to castration-resistant metastases. A minority (25%) of castration-resistant metastatic cases lacked detectable Nestin expression, suggesting that alternate pathways to migration and metastasis may be available to these cells. It will be interesting to look for distinctive intermediate filaments in Nestin-negative cases.

About the origin of Nestin expression in prostate cancer, it may be that Nestin-positive cancer cells are present but so rare in ADT-naive tumors as to be undetectable using the methods used in this study. A more plausible explanation posits a phenotypic shift in already established tumors that coincides with androgen deprivation. The possibility that Nestin expression induces androgen independence can probably be dispensed with, as we never observed Nestin expression in prostate cancers without a prior history of androgen deprivation, whereas androgen deprivation *in vitro* induced Nestin expression (Fig. 1*A*). Instead, our data indicate that androgen deprivation is required to induce a set of cellular adaptations that result in Nestin expression. Our data indicate that the shift to a Nestin-positive lethal phenotype most likely arises at the site of origin, as do other determinants of metastatic potential, despite current difficulties in identifying local selective pressures for their expression (reviewed in ref. 43). Once metastasis has occurred, Nestin expression may provide a selective advantage, as supported by enrichment for Nestin-expressing cells in AT6.3 prostate cancer micrometastases compared with the s.c. xenografts from which they originated (Fig. 4*B*). This and other model systems may be useful for gaining additional insights into the regulation of Nestin expression in cancer, including potential influences of Notch and Hedgehog signaling (28, 30, 31).

Most solid tumors, including prostate cancer, exhibit significant cell to cell heterogeneity with regard to tumor-forming and metastatic potential. Our data (Fig. 5) indicate that, in a significant proportion of prostate cancers, Nestin expression is required for colonizing distant sites in metastasis and thus may be a marker of metastasis initiating "cancer stem cells." In Nestin-expressing prostate cancers, fractionation of Nestin-expressing cells using existing Nestin reporters could shed light on potential relationships between prostate cancer, prostate stem cells, and prostate cancer stem cells.

We have identified a role for the intermediate filament Nestin in migration as a critical component of a novel metastasis pathway in prostate cancer and one that likely operates exclusively in androgen-deprived tumors. Our identification of migration as a Nestin effector function could facilitate further investigation into this pathway and may identify novel points for intervention in metastatic prostate cancer.

Acknowledgments

Received 2/28/2007; revised 6/8/2007; accepted 7/18/2007.

Grant support: NIH grant DK05937, Evensen Family Foundation, and NIH/National Cancer Institute Specialized Program of Research Excellence P50 CA58236 (D.M. Berman and Pathology Core) and German Cancer Aid Foundation Fellowship Grant (W. Kleeberger).

The costs of publication of this article were defrayed in part by the payment of page charges. This article must therefore be hereby marked *advertisement* in accordance with 18 U.S.C. Section 1734 solely to indicate this fact.

We thank N. Abdallah, M. Southerland, and H. Fedor for technical assistance; the Prostate Specimen Repository at the Brady Urological Research Institute at Johns Hopkins for TMAs; D. Danielpour for NRP152 cells; J. Isaacs for AT6.3 cells; and A. De Marzo, P. Coulombe, J. Isaacs, and anonymous reviewers for helpful comments on the manuscript.

References

1. Coulombe PA, Wong P. Cytoplasmic intermediate filaments revealed as dynamic and multipurpose scaffolds. Nat Cell Biol 2004;6:699–706.
2. Lendahl U, Zimmerman LB, McKay RD. CNS stem cells express a new class of intermediate filament protein. Cell 1990;60:585–95.
3. Almqvist PM, Mah R, Lendahl U, Jacobsson B, Hendson G. Immunohistochemical detection of nestin in pediatric brain tumors. J Histochem Cytochem 2002;50:147–58.
4. Berman DM, Karhadkar SS, Hallahan AR, et al. Medulloblastoma growth inhibition by hedgehog pathway blockade. Science 2002;297:1559–61.
5. Dahlstrand J, Collins VP, Lendahl U. Expression of the class VI intermediate filament nestin in human central nervous system tumors. Cancer Res 1992;52: 5334–41.
6. Kobayashi M, Sjoberg G, Soderhall S, Lendahl U, Sandstedt B, Sejersen T. Pediatric rhabdomyosarcomas express the intermediate filament nestin. Pediatr Res 1998;43:386–92.
7. Tsujimura T, Makiishi-Shimobayashi C, Lundkvist J, et al. Expression of the intermediate filament nestin in gastrointestinal stromal tumors and interstitial cells of Cajal. Am J Pathol 2001;158:817–23.
8. Johansson CB, Momma S, Clarke DL, Risling M, Lendahl U, Frisen J. Identification of a neural stem cell in the adult mammalian central nervous system. Cell 1999;96:25–34.
9. Li L, Mignone J, Yang M, et al. Nestin expression in hair follicle sheath progenitor cells. Proc Natl Acad Sci U S A 2003;100:9958–61.
10. About I, Laurent-Maquin D, Lendahl U, Mitsiadis TA. Nestin expression in embryonic and adult human teeth under normal and pathological conditions. Am J Pathol 2000;157:287–95.
11. Frisen J, Johansson CB, Torok C, Risling M, Lendahl U. Rapid, widespread, and longlasting induction of nestin contributes to the generation of glial scar tissue after CNS injury. J Cell Biol 1995;131:453–64.
12. Lin RC, Matesic DF, Marvin M, McKay RD, Brustle O. Re-expression of the intermediate filament nestin in reactive astrocytes. Neurobiol Dis 1995;2:79–85.
13. Niki T, Pekny M, Hellemans K, et al. Class VI intermediate filament protein nestin is induced during activation of rat hepatic stellate cells. Hepatology 1999; 29:520–7.
14. Beachy PA, Karhadkar SS, Berman DM. Tissue repair and stem cell renewal in carcinogenesis. Nature 2004; 432:324–31.
15. Nelson WG, De Marzo AM, DeWeese TL, Isaacs WB. The role of inflammation in the pathogenesis of prostate cancer. J Urol 2004;172:S6–11; discussion S-2.
16. Bova GS, Chan-Tack K, LeCates WW. Lethal metastatic human prostate cancer: autopsy studies and characteristics of metastases. In: Chung LWK, Isaacs WB, Simons JW, editors. Prostate cancer: biology, genetics, and the new therapeutics. Totowa (NJ): Humana Press; 2001. p. 39–60.
17. Lee EC, Tenniswood MP. Emergence of metastatic hormone-refractory disease in prostate cancer after anti-androgen therapy. J Cell Biochem 2004;91:662–70.
18. Navarro D, Luzardo OP, Fernandez L, Chesa N, Diaz-Chico BN. Transition to androgen-independence in prostate cancer. J Steroid Biochem Mol Biol 2002;81: 191–201.
19. Scher HI, Sawyers CL. Biology of progressive, castration-resistant prostate cancer: directed therapies targeting the androgen-receptor signaling axis. J Clin Oncol 2005;23:8253–61.
20. Isaacs JT, Coffey DS. Adaptation versus selection as the mechanism responsible for the relapse of prostatic cancer to androgen ablation therapy as studied in the Dunning R-3327-H adenocarcinoma. Cancer Res 1981; 41:5070–5.
21. English HF, Santen RJ, Isaacs JT. Response of glandular versus basal rat ventral prostatic epithelial cells to androgen withdrawal and replacement. Prostate 1987;11:229–42.
22. Sahlgren CM, Mikhailov A, Hellman J, et al. Mitotic reorganization of the intermediate filament protein nestin involves phosphorylation by cdc2 kinase. J Biol Chem 2001;276:16456–63.
23. Chou YH, Khuon S, Herrmann H, Goldman RD. Nestin promotes the phosphorylation-dependent disassembly of vimentin intermediate filaments during mitosis. Mol Biol Cell 2003;14:1468–78.
24. Steinert PM, Chou YH, Prahlad V, et al. A high molecular weight intermediate filament-associated protein in BHK-21 cells is nestin, a type VI intermediate filament protein. Limited co-assembly *in vitro* to form heteropolymers with type III vimentin and type IV α-internexin. J Biol Chem 1999;274:9881–90.
25. Sahlgren CM, Pallari HM, He T, Chou YH, Goldman RD, Eriksson JE. A nestin scaffold links Cdk5/p35 signaling to oxidant-induced cell death. EMBO J 2006;25: 4808–19.
26. Danielpour D, Kadomatsu K, Anzano MA, Smith JM, Sporn MB. Development and characterization of nontumorigenic and tumorigenic epithelial cell lines from rat dorsal-lateral prostate. Cancer Res 1994;54: 3413–21.
27. Deutsch EW, Ball CA, Bova GS, et al. Development of the minimum information specification for *in situ* hybridization and immunohistochemistry experiments (MISFISHIE). OMICS 2006;10:205–8.
28. Karhadkar SS, Bova GS, Abdallah N, et al. Hedgehog signalling in prostate regeneration, neoplasia and metastasis. Nature 2004;431:707–12.
29. Cheung AM, Brown AS, Hastie LA, et al. Three-dimensional ultrasound biomicroscopy for xenograft growth analysis. Ultrasound Med Biol 2005;31:865–70.
30. Watkins DN, Berman DM, Burkholder SG, Wang B, Beachy PA, Baylin SB. Hedgehog signalling within airway epithelial progenitors and in small-cell lung cancer. Nature 2003;422:313–7.
31. Gipp J, Gu G, Crylen C, Kasper S, Bushman W. Hedgehog pathway activity in the LADY prostate tumor model. Mol Cancer 2007;6:19.
32. Mokry J, Cizkova D, Filip S, et al. Nestin expression by newly formed human blood vessels. Stem Cells Dev 2004;13:658–64.
33. Freedland SJ, Humphreys EB, Mangold LA, et al. Risk of prostate cancer-specific mortality following biochemical recurrence after radical prostatectomy. JAMA 2005;294:433–9.
34. Dong JT, Lamb PW, Rinker-Schaeffer CW, et al. KAI1, a metastasis suppressor gene for prostate cancer on human chromosome 11p11.2. Science 1995;268: 884–6.
35. Webb DJ, Parsons JT, Horwitz AF. Adhesion assembly, disassembly and turnover in migrating cells—over and over and over again. Nat Cell Biol 2002;4:E97–100.
36. Yamaguchi H, Wyckoff J, Condeelis J. Cell migration in tumors. Curr Opin Cell Biol 2005;17:559–64.
37. Gilles C, Polette M, Zahm JM, et al. Vimentin contributes to human mammary epithelial cell migration. J Cell Sci 1999;112:4615–25.
38. Hendrix MJ, Seftor EA, Chu YW, Trevor KT, Seftor RE. Role of intermediate filaments in migration, invasion and metastasis. Cancer Metastasis Rev 1996; 15:507–25.
39. Bellin RM, Huiatt TW, Critchley DR, Robson RM. Synemin may function to directly link muscle cell intermediate filaments to both myofibrillar Z-lines and costameres. J Biol Chem 2001;276:32330–7.
40. Esni F, Stoffers DA, Takeuchi T, Leach SD. Origin of exocrine pancreatic cells from nestin-positive precursors in developing mouse pancreas. Mech Dev 2004;121: 15–25.
41. Means AL, Meszoely IM, Suzuki K, et al. Pancreatic epithelial plasticity mediated by acinar cell transdifferentiation and generation of nestin-positive intermediates. Development 2005;132:3767–76.
42. Doles J, Cook C, Shi X, Valosky J, Lipinski R, Bushman W. Functional compensation in Hedgehog signaling during mouse prostate development. Dev Biol 2006;295: 13–25.
43. Gupta PB, Mani S, Yang J, Hartwell K, Weinberg RA. The evolving portrait of cancer metastasis. Cold Spring Harb Symp Quant Biol 2005;70:291–7.